

Entropy amplification from energy feedback in simulated galaxy groups and clusters

S. Borgani^{1,2}, A. Finoguenov³, S.T. Kay^{4,5}, T.J. Ponman⁶, V. Springel⁷,
 P. Tozzi⁸, G.M. Voit⁹

¹ Dipartimento di Astronomia dell’Università di Trieste, via Tiepolo 11, 34131 Trieste, Italy (borgani@ts.astro.it)

² INFN – National Institute for Nuclear Physics, Trieste, Italy

³ Max-Planck-Institut für extraterrestrische Physik, Giessenbachstrasse, 85748 Garching, Germany (alexis@xray.mpe.mpg.de)

⁴ Astronomy Centre, Department of Physics and Astronomy, University of Sussex, Brighton BN1 9QH, UK

⁵ Astrophysics, Keble Road, Oxford OX1 3RH, UK (skay@astro.ox.ac.uk)

⁶ School of Physics and Astronomy, University of Birmingham, Edgbaston, Birmingham B15 2TT, UK (tjp@star.sr.bham.ac.uk)

⁷ Max-Planck-Institut für Astrophysik, Karl-Schwarzschild Strasse 1, Garching bei München, Germany (volker@mpa-garching.mpg.de)

⁸ INAF – Osservatorio Astronomico di Trieste, via Tiepolo 11, 34131 Trieste, Italy (tozzi@ts.astro.it)

⁹ Department of Physics and Astronomy, Michigan State University, BPS Building, East Lansing, MI 48824, USA (voit@pa.msu.edu)

21 September 2018

ABSTRACT

We use hydrodynamical simulations of galaxy clusters and groups to study the effect of pre-heating on the entropy structure of the intra-cluster medium (ICM). Our simulations account for non-gravitational heating of the gas either by imposing a minimum entropy floor at redshift $z_h = 3$ in adiabatic simulations, or by considering feedback by galactic winds powered by supernova (SN) energy in runs that include radiative cooling and star formation. In the adiabatic simulations we find that the entropy is increased out to the external regions of the simulated halos as a consequence of the transition from clumpy to smooth accretion induced by extra heating. This result is in line with the predictions of the semi-analytical model by Voit et al. However, the introduction of radiative cooling substantially reduces this entropy amplification effect. While we find that galactic winds of increasing strength are effective in regulating star formation, they have a negligible effect on the entropy profile of cluster-sized halos. Only in models where the action of the winds is complemented with diffuse heating corresponding to a pre-collapse entropy do we find a sizable entropy amplification out to the virial radius of the groups. Observational evidence for entropy amplification in the outskirts of galaxy clusters and groups therefore favours a scenario for feedback that distributes heating energy in a more diffuse way than predicted by the model for galactic winds from SN explosions explored here.

Key words: Cosmology: numerical simulations – galaxies: clusters – hydrodynamics – X-ray: galaxies

1 INTRODUCTION

The thermodynamic properties of the intra-cluster medium (ICM) reflect the full history of the cosmic evolution of baryons. This evolution is primarily driven by gravity, which shapes the gas distribution on large scales and determines the hierarchical assembly of cosmic structures, but also by a complex interplay with the hydrodynamic processes of star formation and galaxy evolution (see Rosati et al. 2002; Voit 2005 for recent reviews, and references therein). Due to the high density and temperature reached by gas in the environment of galaxy clusters and groups, X-ray observations

provided so far the most powerful diagnostics on its thermal properties.

The simplest model for the evolution of the ICM accounts only for the action of gravity (Kaiser 1986). This picture is said to be self-similar because it predicts that galaxy groups and clusters of different richness are essentially scaled versions of each other. Based on this realization, one can then derive unique scaling relations between X-ray observables. For instance, the X-ray luminosity, L_X , should scale with the gas temperature T as $L_X \propto T^2$; the “entropy” $S = T/n_e^{2/3}$ (n_e is the electron number density) should scale linearly with temperature owing to the self-similarity of the

gas density profiles. Furthermore, spherical gas accretion in a NFW halo (Navarro, Frenk & White 1997) predicts entropy to scale with the cluster-centric distance as $S \propto R^{1.1}$ (Tozzi & Norman 2001).

While adiabatic hydrodynamical simulation of clusters have validated this simple picture (e.g., Navarro et al. 1995; Eke et al. 1998; Borgani et al. 2001), a number of observations have now established that gravity cannot be the only player: the gas density profiles in the central regions of groups and poor clusters are observed to be shallower than in the self-similar model, and the relative entropy level is correspondingly higher than in rich clusters (e.g., Ponman et al. 1999; Finoguenov et al. 2002; Ponman et al. 2003). As a consequence, smaller systems are relatively underluminous, thus producing too steep an L_X – T relation, $L_X \propto T^{3.5}$ (e.g., Markevitch 1998; Arnaud & Evrard 1999; Sanderson et al. 2003).

These observational facts call for additional physics in the form of non-gravitational processes, capable of breaking the self-similarity of the ICM properties. As a solution, a number of authors have proposed the presence of extra heating, possibly occurring before the cluster collapse (e.g. Evrard & Henry 1991; Kaiser 1991; Bower 1997; Cavaliere, Menci & Tozzi 1998; Balogh et al. 1999; Bialek, Evrard & Mohr 2001; Tozzi & Norman 2001; Borgani et al. 2002; Dos Santos & Doré 2002), or of radiative cooling (e.g., Bryan 2000; Voit & Bryan 2001; Wu & Xue 2002), or, perhaps more likely, of a combination of these two effects (e.g., Voit et al. 2002; Muanwong et al. 2002; Tornatore et al. 2003; Borgani et al. 2004; Kay et al. 2003, 2004). Radiative cooling determines the minimum entropy level of the X-ray emitting gas through a selective removal of gas with short cooling time. On the other hand, non-gravitational heating affects the amount of gas which can cool down to form stars, thereby preventing a cooling runaway. Independent of the details of the model and the nature of the assumed heating energy, it has been common prejudice that the ICM entropy would only be affected in the central regions of clusters, while the self-similarity would be preserved in the halo outskirts, where dynamics is still dominated by gravity.

However, based on a semi-analytic model for gas accretion in clusters, Voit et al. (2003) have recently predicted that a smoothing of the gas density due to preheating in infalling sub-halos would boost the entropy production at the accretion shock of clusters. As a result, an excess of entropy with respect to the prediction of the self-similar model is generated in the cluster outskirts. This effect due to smooth accretion should be more important for poorer systems, since their accretion is dominated by smaller clumps which are more affected by pre-heating. Therefore, entropy generation is expected to be more efficient in smaller systems, thus boosting their entropy profiles more than those of more massive structures.

Observational support for this model has been provided by Ponman et al. (2003). Using ROSAT/ASCA data for a large set of clusters and groups, they found that the entropy level in the outskirts is higher than predicted by self-similar scaling, in fact by a larger amount for poorer systems. Ponman et al. (2003) also gave a possible interpretation in terms of smoothing of the accretion pattern, concentrating on the effect of smoothing on accreting filaments rather than on gas clumps. The lack of self-similar scaling for the overall nor-

malisation of the entropy profiles has also been confirmed by Pratt & Arnaud (2004) and Piffaretti et al. (2005), based on *XMM-Newton* observations, and by Mushotzky et al. (2003) from Chandra data. Thanks to the possibility to perform spatially resolved spectroscopy, these authors were able to derive the entropy profiles from the actual temperature profiles. Consistent with the results by Ponman et al. (2003), they concluded that the shape of the entropy profiles appears to be quite similar for all systems, with an amplitude that follows the scaling $S \propto T^{2/3}$ more closely than the $S \propto T$ scaling expected from self-similarity.

The question then arises as to whether the observed entropy structure of groups and clusters can be used to derive information on the nature of the feedback that affects the thermodynamical history of cosmic baryons. Whatever the astrophysical source of this feedback is, it must act in such a way as to regulate star formation and, at the same time, to reproduce the observed entropy profiles.

Based on the model of star formation and supernova (SN) feedback by Springel & Hernquist (2003a, SH03 hereafter), Borgani et al. (2004) performed a large cosmological hydrodynamical simulation with the aim of studying the X-ray properties of galaxy clusters and groups. Although the model provides a realistic description of the cosmic star formation history (Springel & Hernquist 2003b), clusters are found to have approximately self-similar entropy profiles, which is not consistent with observations. This result demonstrates that generating the required level of entropy amplification at cluster outskirts is a challenging task for hydrodynamical simulations even if they treat star formation and feedback. A number of simple feedback schemes have been suggested that heat the gas surrounding galaxies in order to better reproduce the observed entropy scaling (e.g. Kay et al. 2004). While such experiments provide very useful guidelines, it is clear that a self-consistent numerical implementation of a physically well motivated feedback model which can successfully satisfy a large body of observational constraints is highly desirable.

In this paper, we use hydrodynamical simulations to explore a suite of different heating schemes, both for radiative and non-radiative runs. We focus on four objects which cover the mass range from poor clusters to poor groups. The aim of our analysis is to verify whether an appreciable entropy amplification at large radii, as predicted by Voit et al. (2003), can be obtained with simple preheating schemes and/or with self-consistent models that include feedback from SN-driven galactic winds.

The main questions that we intend to address with our analysis are the following: (a) Is the entropy amplification by smoothed accretion confirmed by hydrodynamical simulations when a simple scenario for pre-heating with an entropy floor is invoked? (b) Does this effect persist when simulations include a realistic treatment for star formation and SN feedback? (c) What are the observed entropy profiles telling us about the nature of the feedback that affects the evolution of the ICM and IGM?

The outline of this paper is as follows. In Section 2, we describe the simulations that we carried out and the different schemes to provide non-gravitational heating. Section 3 is devoted to the presentation and discussion of the results, both for the non-radiative and for the radiative runs. In Section 4, we summarise our results and give our conclusions.

2 THE SIMULATIONS

Our simulations have been carried out with GADGET-2, a new version of the parallel Tree-SPH code GADGET (Springel, Yoshida & White 2001). It uses an entropy-conserving formulation of SPH (Springel & Hernquist 2002), and includes radiative cooling/heating by a uniform evolving UV background, a sub-resolution description of star formation from a multiphase interstellar medium, and the effect of galactic winds powered by SN energy feedback (SH03).

The simulated groups and clusters are the same as in Tornatore et al. (2003) and Finoguenov et al. (2003), and we refer to these papers for more details on their characteristics. Our set of simulated objects includes a moderately rich cluster with $M_{\text{vir}} \simeq 2.6 \times 10^{14} h^{-1} M_{\odot}$, and three groups-sized objects having virial mass in the range $1.6 \times 10^{13} \lesssim M_{\text{vir}}/(h^{-1} M_{\odot}) \lesssim 4.2 \times 10^{13}$. The corresponding halos have been selected from a DM-only simulation of a Λ CDM model with $\Omega_m = 0.3$, $h = 0.7$, $\sigma_8 = 0.8$ and $f_{\text{bar}} = 0.13$ for the baryon fraction, within a box of size $70 h^{-1} \text{Mpc}$. As such, they encompass the mass range characteristic of moderately rich clusters to groups, where the effect of non-gravitational heating is expected to be important.

Using a re-simulation technique, the mass and force resolution has been increased in the Lagrangian regions of the parent box which correspond by $z = 0$ to volumes encompassing several virial radii around each of the selected halos. The resolution is progressively degraded in regions farther away, allowing us to save computing time while still providing an accurate representation of the large-scale tidal field. In the high resolution region of the cluster simulation, gas particles have mass $m_{\text{gas}} \simeq 2.2 \times 10^8 h^{-1} M_{\odot}$, and we chose $\epsilon_{\text{Pl}} = 5 h^{-1} \text{kpc}$ for the Plummer-equivalent softening scale, kept fixed in physical units out to $z = 2$, and then fixed in co-moving units at earlier times. In order to have a comparable number of particles within the virial regions of the different simulated structures, we increased the mass resolution by a factor of eight for the runs of the groups and, correspondingly, we decreased the force softening by a factor of two. The main characteristics of the simulations are listed in Table 1.

We have simulated each object both with radiative and non-radiative physics. Our non-radiative runs include the case of purely gravitational heating (GH) and two pre-heating models, which are implemented by imposing a minimum gas entropy of $S_{\text{fl}} = 25$ and 100 keV cm^2 at redshift $z_h = 3$, respectively. Entropy of heated particles is raised by increasing their internal energy (i.e., temperature), while leaving their density unchanged. For the radiative runs, we have performed several simulations by changing either the parameters controlling the galactic winds or the level of the pre-heating entropy floor. In the model of SH03, the velocity of the galactic winds, v_w , scales with the fraction η of the SN-II feedback energy that contributes to the winds, as $v_w \propto \eta^{1/2}$ (see eq.[28] in SH03). The total energy provided by SN-II is computed by assuming that they are due to exploding stars with mass $> 8 M_{\odot}$, each SN releasing 10^{51} ergs , and that their abundance is given by a Salpeter (1955) initial mass function (IMF). In our simulations, we consider the cases $\eta = 0.5, 1$ and 3 , yielding $v_w \simeq 340, 480$ and 840 km s^{-1} (runs W1, W2 and W3), respectively. While

Table 1. Physical characteristics and numerical parameters of the simulated halos. Column 2: total mass within the virial radius at $z = 0$ ($10^{13} h^{-1} M_{\odot}$); Column 3: virial radius ($h^{-1} \text{Mpc}$); Column 4: mass-weighted temperature within R_{vir} (keV); Column 5: mass of the gas particles in the simulations ($10^8 h^{-1} M_{\odot}$); Column 6: Plummer-equivalent gravitational softening at $z = 0$ ($h^{-1} \text{kpc}$). The numbers reported in Columns 2-4 refer to the non-radiative run with gravitational heating (GH) only, but their values do not significantly change for the other runs.

Run	M_{vir}	R_{vir}	T_{vir}	m_{gas}	ϵ
Cluster	26.4	1.31	2.04	2.17	5.0
Group-1	4.17	0.71	0.52	0.27	2.5
Group-2	1.75	0.53	0.39	0.27	2.5
Group-3	1.64	0.52	0.28	0.27	2.5

assuming $\eta > 1$ is clearly unrealistic in this picture, it can be phenomenologically interpreted as being due to an extra energy source, e.g. coming from a top-heavier IMF or from an AGN component.

In their model for galactic winds, SH03 treated SPH particles that become part of the wind as temporarily decoupled from hydrodynamical interactions, in order to allow the wind particles to leave the dense interstellar medium without disrupting it. This decoupling is regulated by two parameters. The first parameter, ρ_{dec} , defines the minimum density the wind particles can reach before being coupled again. If ρ_{th} is the threshold gas density for the onset of star formation ($\rho_{\text{th}} \simeq 2.8 \times 10^{-25} \text{ g cm}^{-3}$ in the SH03 model), then it should be $\rho_{\text{dec}} < \rho_{\text{th}}$ for the winds to leave the star-forming region, and the typical setting by SH03 has been $\rho_{\text{dec}} = 0.1 - 1.0 \rho_{\text{th}}$. The second parameter, l_{dec} , provides a maximum time via $t_{\text{dec}} = l_{\text{dec}}/v_e$ a wind particle may travel freely before becoming hydrodynamically coupled again. If this time has elapsed, the particle is coupled again, even if it has not yet reached ρ_{dec} . The l_{dec} parameter is introduced only to ensure that the decoupling is stopped quickly also in cases where the wind particle cannot escape the dense ISM due to gravity alone. We provide the values of ρ_{dec} and l_{dec} used for the radiative runs in Table 2. The W1, W2 and W3 models all have the same values for these parameters, but they differ in their wind velocity. In an attempt to produce more widely distributed by winds, we have also run an additional model W4 which has the same wind speed as W3, but where we allowed the winds to reach much lower densities and larger distances while being decoupled.

In summary, we have performed 9 runs for each of the four simulated structures, corresponding to different ways of changing the gas physics. The characteristics of these runs are given in Table 2. We also provide in this table the mean value of non-gravitational specific energy assigned to the gas that falls at the end of the run within the virial radius of the cluster (comparable amounts are found for the three groups). For the simulations with pre-heating, we have determined this energy by tracking back to $z = 3$ all the gas particles within R_{vir} at $z = 0$ and summing up the energy contributions required to increase their entropy to the floor value where needed. For the runs including SN feedback, we measure the total stellar mass within R_{vir} at $z = 0$ and we compute the total number of SN-II expected for the assumed Salpeter IMF. The resulting energy is then multiplied

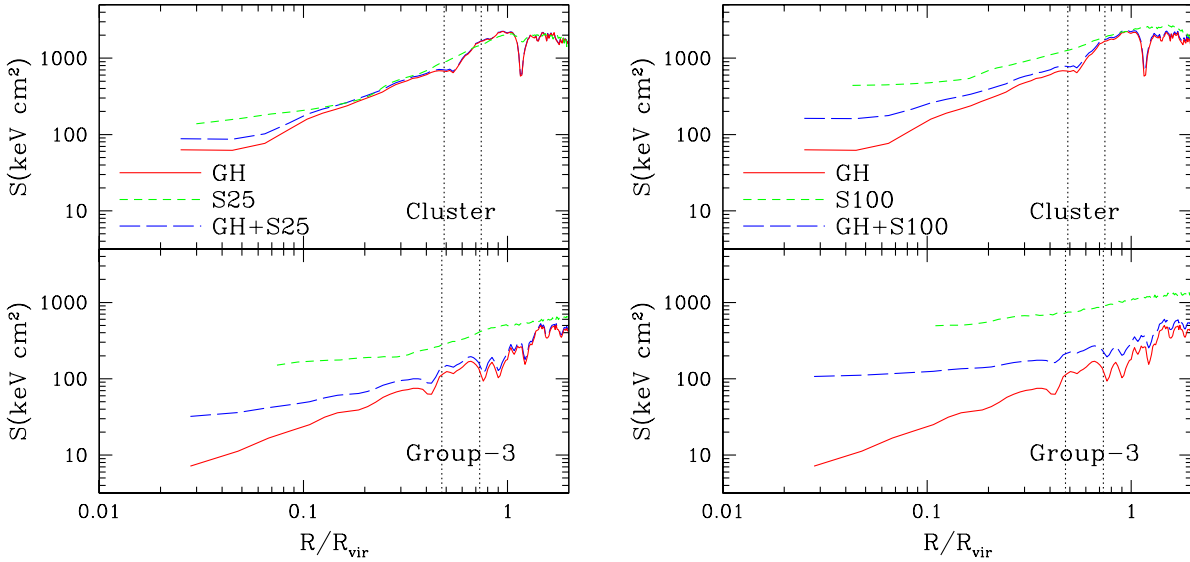


Figure 1. Entropy profiles of the non-radiative simulations. In the left and in the right panels, we compare the results for the gravitational-heating (GH) runs (solid curves) to those for the pre-heated runs (short-dashed curves) with entropy floor $S_{\text{fl}} = 25$ keV cm 2 (S25) and $S_{\text{fl}} = 100$ keV cm 2 (S100), respectively (see Table 2). Upper and lower panels correspond to the simulations of the Cluster and of the Group-3. In each panel, we also show with a long-dashed curve the entropy profile obtained by adding the entropy-floor value, S_{fl} , to the GH case. The difference between the short-dashed and the long-dashed curves provides the net entropy amplification. The two vertical dotted lines mark the positions of R_{200} and R_{500} , defined as the radii encompassing an average density $200\rho_{\text{cr}}$ and $500\rho_{\text{cr}}$, respectively (here ρ_{cr} is the critical cosmic density).

Table 2. Description of the different runs. Column 1: run name; Column 2: level of the entropy floor at $z_h = 3$ (keV cm 2); Column 3: wind speed (km s $^{-1}$); Column 4: specific heating energy assigned to the gas particles that fall within R_{vir} at $z = 0$ (keV/particle); Column 5: the limiting density for wind decoupling (in units of the threshold density, ρ_{th} , for star formation (see text)); Column 6: the maximum length that winds travel while being decoupled (units of h^{-1} kpc); Column 7: fraction of baryons in stars within R_{vir} . The values in Columns 4 and 7 refer to the simulations of the Cluster.

Run	S_{fl}	v_w	E_h	ρ_{dec}	d_{dec}	f_*
Non-rad. runs						
GH						
S25	25		0.5			
S100	100		2.2			
Rad. runs						
W1		341	0.3	0.5	10	0.20
W2		484	0.5	0.5	10	0.17
W3		837	1.2	0.5	10	0.14
W4		837	1.1	0.01	50	0.12
W1+S25	25	341	0.2+0.4 †	0.5	10	0.13
W1+S100	100	341	0.2+1.8 †	0.5	10	0.13

† We report separately the energy budget associated to galactic winds (see text) and the pre-heating energy required at $z = 3$ to establish the entropy floor.

by the efficiency parameter η to compute the total energy associated with wind feedback.

Looking at Table 2, we note that the heating energy required to create the entropy floors is comparable to those of the winds. However, the way in which these two feedback

schemes affect the thermodynamics of the diffuse baryons is intrinsically very different. The first heating mechanism provides a diffuse energy input that can in principle reach all the gas particles in the simulations, and is provided in an impulsive way (i.e. all the energy is released at the heating redshift $z_h = 3$). The second mechanism, instead, releases energy gradually in time, since it follows the pattern of star formation, and it is narrowly concentrated around star-forming regions. As we will discuss in the following, these differences have an important impact on the smoothing of the accretion pattern and, therefore, on the entropy generation by accretion shocks.

3 RESULTS

3.1 Non-radiative runs

In Figure 1, we compare the effect of imposing the two different entropy floors on the entropy profiles of the cluster simulation and of ‘Group-3’. Here and in the following we plot profiles to an innermost radius which contains 100 SPH particles. This radius has been shown to be the smallest one where numerically converged results for the X-ray luminosity can be obtained (Borgani et al. 2002).

As expected, the effect of pre-heating is that of increasing the level of the ICM entropy by a larger amount for the less massive system, an effect that increases in strength for a higher entropy floor. The runs with gravitational heating display a number of wiggles which mark the positions of merging sub-halos carrying low-entropy gas. These wiggles are erased once the gas is pre-heated. This is consistent with

the expectation that pre-heating destroys the gas content of halos whose virial temperature is lower than the specific pre-heating energy. In the cluster run, the entropy increase due to pre-heating is marginal at the virial radius, thus implying that the overall ICM thermal energy content within R_{vir} is mainly determined by the action of gravity.

In Figure 2, we provide further information about the effect of pre-heating on the entropy structure of the ICM. Here we show the entropy-density phase diagram of gas particles. The two separate concentrations of points mark the gas particles falling within $0.1 R_{\text{vir}}$ and those having cluster-centric distances in the range $(0.9 - 1.1) R_{\text{vir}}$, the former being those having larger densities. Following these two populations of gas particles allows us to understand the different effects that non-gravitational physics has in the innermost and in the outskirt regions of the ICM. In the outer cluster regions in the GH runs (left panels), the change of slope in the $S - \rho_g$ relation marks the transition from diffuse (shocked) accretion to clumpy accretion (see also Sect. 3.2 and Figure 5 below). The clumpy accretion is associated with merging subgroups and filaments, which are characterised by low entropy and high density, and are erased by pre-heating with an entropy floor of 100 keV cm^2 (S100 runs, right panels). This demonstrates that the effects of pre-heating are: (a) to cancel any signature of clumpy accretion in the outskirts; (b) to suppress the gas density in the central halo regions, and (c) to amplify the entropy of both the diffuse phase in the outer regions and of the gas in the central regions, by an amount that increases for lower-mass systems.

In their semi-analytic description of entropy generation from diffuse accretion, Voit et al. (2003) have shown that the post-shock gas entropy is higher than it would be without preheating, at a given density, by an amount between $0.84 S$ and S , where S is the added entropy. Therefore, when comparing the profiles of preheated simulations to the corresponding GH profiles where the preheating entropy level is simply added to it, any excess entropy should then be attributed to the amplification effect due to accretion of smoothed gas instead of clumps. We expect this effect to become more prominent for stronger pre-heating, which makes the accretion more diffuse, and for smaller groups, where the accretion is dominated by comparatively smaller gas clumps. In Fig. 1, the long-dashed curves show the profiles obtained by adding the floor value, S_{fl} , to the GH profile. Consistent with the expectation from the model by Voit et al. (2003), we find clear evidence for the entropy amplification effect. It is more apparent for the higher entropy floor and for the smaller halo of the Group-3. For instance, at $R = 0.1 R_{\text{vir}}$, we obtain for the cluster simulations an amplification of 14 per cent and 84 per cent for the S25 and S100 runs, respectively. These numbers increase to about 230 per cent and 300 per cent, respectively, for the ‘Group-3’ runs.

We note that our pre-heating scheme does not increase the entropy of each gas particle by a fixed extra amount. Instead, it creates an entropy floor, so that the extra entropy assigned to each particle can be zero if the particle is already at high entropy, or just the value required to attain the floor value. On the other hand, the model by Voit et al. (2003) is a prediction for the entropy amplification when pre-heating is implemented by adding a constant amount of entropy to all gas particles. In this case, we would have obtained a stronger

pre-heating and, therefore, an even stronger amplification effect.

The signature of differential entropy amplification extending out to outer regions of groups and clusters is in line with observational evidences based both on ROSAT/ASCA (e.g. Ponman et al. 2003) and XMM-Newton data (e.g. Pratt & Arnaud 2004; Piffaretti et al. 2005). However, despite the trend of progressively higher relative entropy levels in groups, the observational data also indicates that the shape of entropy profiles is almost independent of mass, with no evidence for the presence of large isentropic cores. This is quite different from the behaviour seen in our non-radiative simulations, where an amplification of entropy at the cluster outskirts is obtained at the price of creating much flatter entropy profiles in groups and larger isentropic cores than in clusters (see Fig. 1).

3.2 Simulations with radiative cooling

The results for the entropy profiles change substantially for the radiative runs. In Figure 3, we compare the profiles for the simulations including cooling and star formation, obtained by either changing the parameters of the winds (left panels) or by adding a pre-heating entropy floor to the feedback of the W1 model. As for the ‘Cluster’, increasing the wind speed leaves the entropy profiles completely unaffected in the halo outskirts. As for the central regions, increasing the wind speed from the W1 to the W2 model slightly decreases the entropy level. In fact, the stronger feedback creates a population of lower entropy particles which are kept in the hot phase by the larger amount of energy feedback, instead of cooling down. Further increasing the wind speed (W2 and W3 runs) or changing the parameters defining the wind decoupling do not further change the entropy profile for the Cluster.

Although the effect of stronger winds is more apparent for the ‘Group-3’ run, it is nevertheless still marginal for $R \gtrsim 0.5 R_{\text{vir}}$. However, increasing the wind speed has a significant effect on the entropy profile in the inner regions of ‘Group-3’: the stronger feedback creates a nearly isentropic regime for $0.07 \lesssim R/R_{\text{vir}} \lesssim 0.5$, while the profile steepens again in the innermost regions, where cooling starts to dominate. Quite intriguingly, a similar behaviour has been recently found by Mahdavi et al. (2005), based on an analysis of galaxy groups observed with XMM-Newton. They find entropy profiles with a broken power-law shape $S \propto R^\alpha$, with an inner and outer slope of $\simeq 0.9$ and $\simeq 0.4$, respectively, and a transition that takes place at about $0.1 R_{500}$. We also note that the presence of a strong wind reduces the resulting fraction of stars from about 20 per cent to about 13 per cent (see Table 2). On one hand this demonstrates that strong winds do increase entropy and, therefore, the cooling time of the gas surrounding star-forming regions (e.g., Springel & Hernquist 2003b; Borgani et al. 2004, in preparation). On the other hand, the results shown in the left panels of Fig. 3 also indicate that this effect is not causing a transition from clumpy to diffuse accretion, as would be required to generate an entropy amplification effect.

Allowing the wind particles to be decoupled until they reach lower densities, and hence allowing them to travel to a larger distance from the star-forming regions before interacting with the diffuse gas (model W4), only produces a

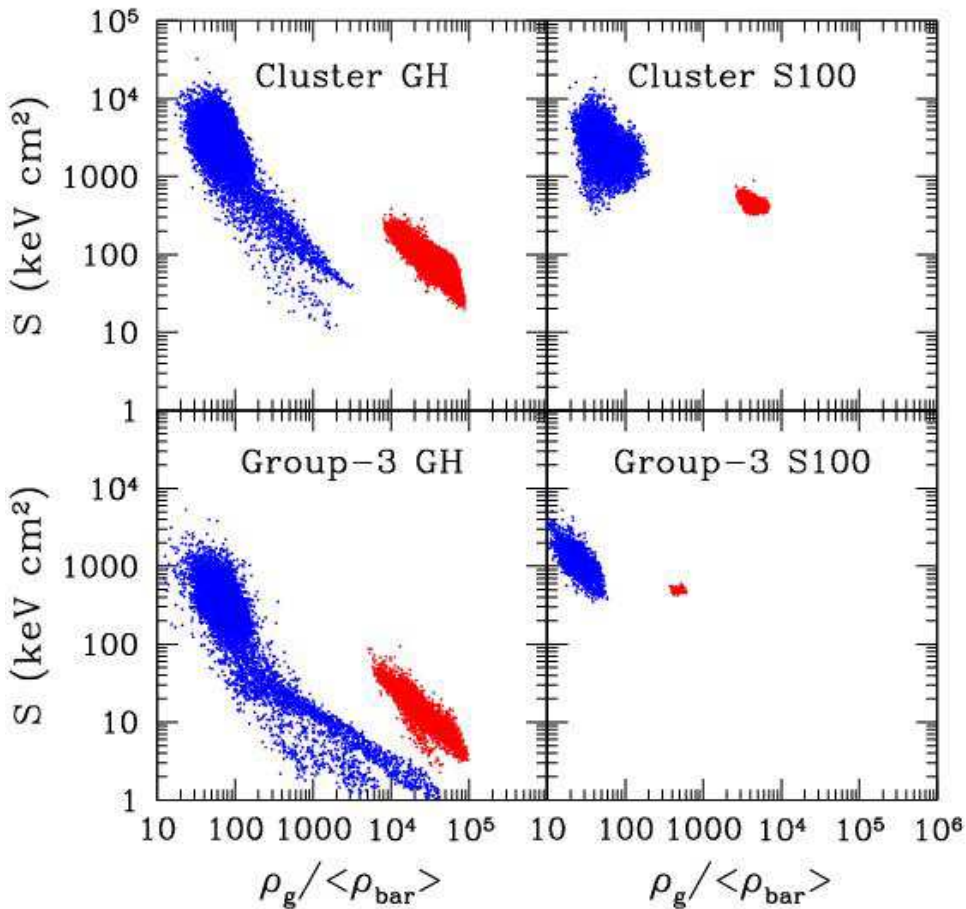


Figure 2. The entropy–density phase diagram for the runs with gravitational heating only (GH, left panels) and with pre–heating with an entropy floor of 100 keV cm² (S100, right panel). Upper and lower panels refer to the Cluster and to the Group-3, respectively. The gas density is given in units of the mean density of cosmic baryons. The concentration of (red) points in the lower right part of each panel is for the gas particles within 0.1 R_{vir} , while the concentration of (blue) points starting from the upper left part of each panel is for the gas particles found between 0.9 R_{vir} and 1.1 R_{vir} .

modest change. Since the mechanical wind energy is thermalized at lower gas densities in this model, radiative losses are reduced as a consequence of longer cooling times. However, the resulting additional suppression of star fraction (see Table 2) and increase of the entropy in the ‘Group-3’ simulation are too small to change our conclusions.

These results on the effect of winds are also supported by the phase–diagrams shown in Figure 4, by the relative distribution of low–entropy and high–entropy particles in the halo outskirts, shown in Figure 5, and by the maps of gas density of the ‘Cluster’ runs, shown in Figure 6. The latter demonstrates that both in the proto–cluster region at $z = 2$ and in the cluster at $z = 0$, the stronger winds wash out only the smallest halos and make the larger ones slightly puffier, while preserving the general structure of the cosmic web surrounding the Lagrangian cluster region.

By comparing the results of the W1 and W3 models in Figs. 4 and 5 (left and central panels, respectively), we see that a higher wind speed has also a negligible effect on the Cluster, despite being able to erase accreting clumps in the outskirts and to push the gas in the central regions of the

‘Group-3’ simulation to higher entropy. In all cases, we find that the stronger winds of the W3 and W4 models are quite ineffective in increasing the entropy of the diffusely accreting gas.

A larger effect on the ICM entropy structure is induced by adding a pre–heating entropy floor to the W1 feedback (right panels of Fig. 3). In this case, a sizable amplification is obtained for both the ‘Group-3’ and the ‘Cluster’ simulations, at least when the higher entropy floor, $S_{\text{f}} = 100$ keV cm², is used. As shown in Fig. 6, this entropy amplification is associated with a much smoother gas density distribution, both at $z = 2$ and at $z = 0$. In this case, the filamentary structure of the gas distribution is completely erased, while only the largest halos are able to retain part of their gas content. This visually demonstrates that a transition from clumpy to smooth accretion during the process of cluster formation requires a more broadly distributed form of feedback.

The effect on the S – ρ_g phase diagram is shown in the right panels of Fig. 4: Adding the entropy floor has a stronger impact in smoothing the pattern of gas accretion than in

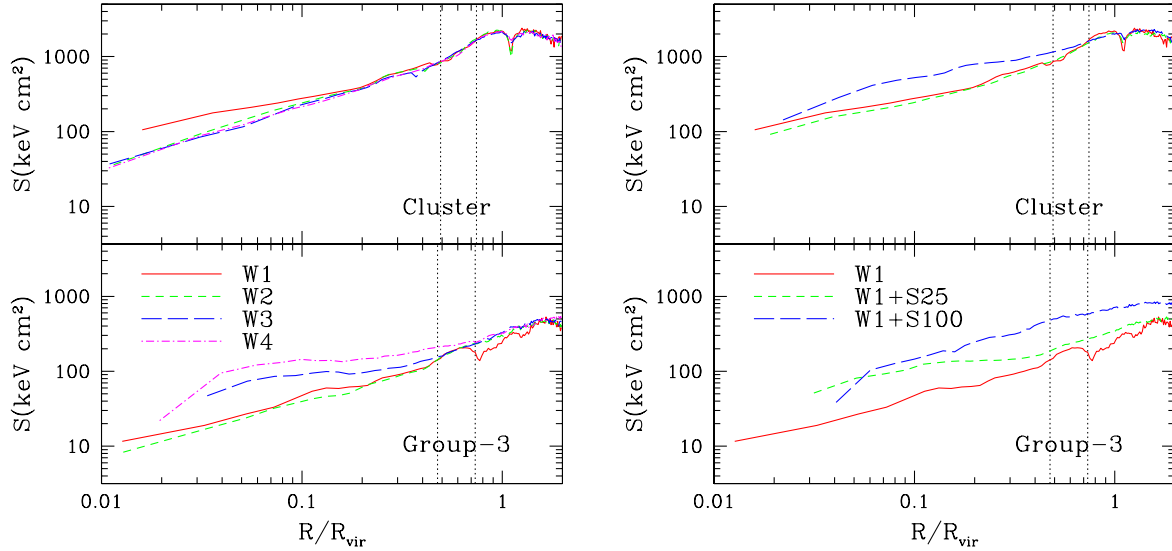


Figure 3. Entropy profiles of the radiative simulations. The left and the right panels show the effect of changing the velocity of the galactic winds and of pre-heating with an entropy floor, respectively. Results for the Cluster and for the Group-3 are shown in the upper and lower panels, respectively. The solid curves always indicate the model W1 with $v_w = 341 \text{ km s}^{-1}$. In the left panels, the short-dashed and long-dashed curves are for $v_w = 484$ and 720 km s^{-1} (W2 and W3 models), respectively, while the dot-dashed curves are for the runs with different values for the parameters defining the wind decoupling (W4 model, see text). In the right panels, short-dashed and long-dashed curves are for the W1 runs with entropy floors of 25 and 100 keV cm^2 (models W1+S25 and W1+S100), respectively. The vertical dotted lines have the same meaning as in Fig.1.

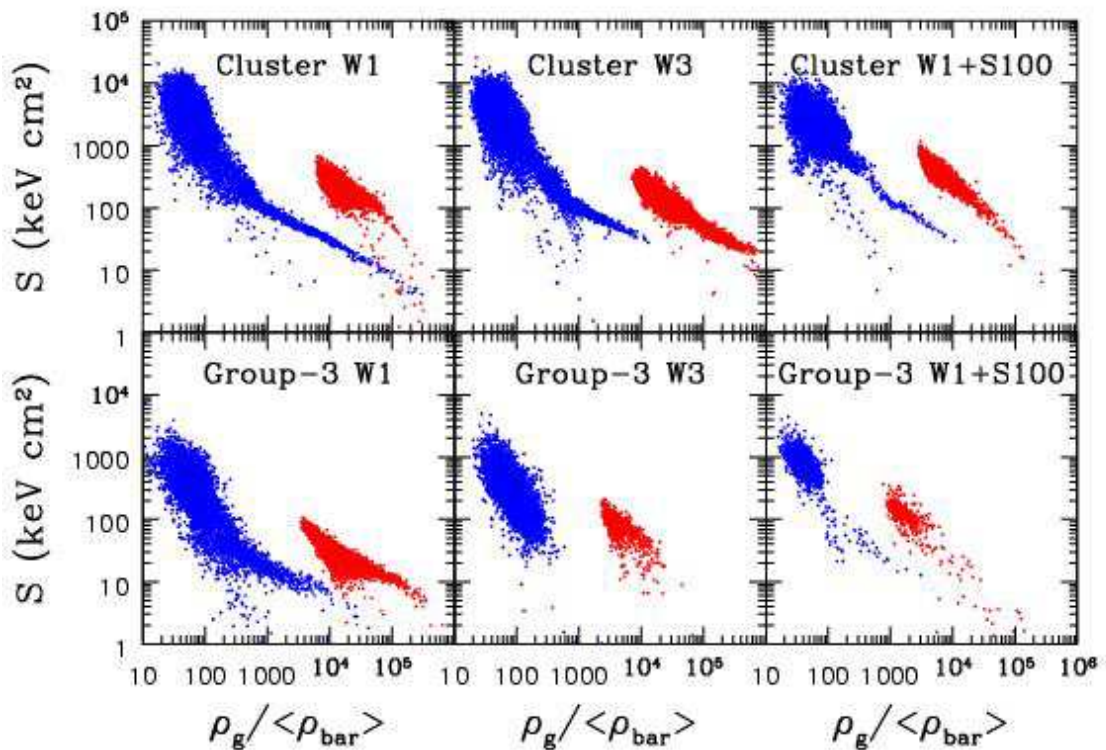


Figure 4. The same as in Figure 2, but for the radiative runs. Left, central and right panels are for the W1, W3 and W1+S100 runs, respectively.

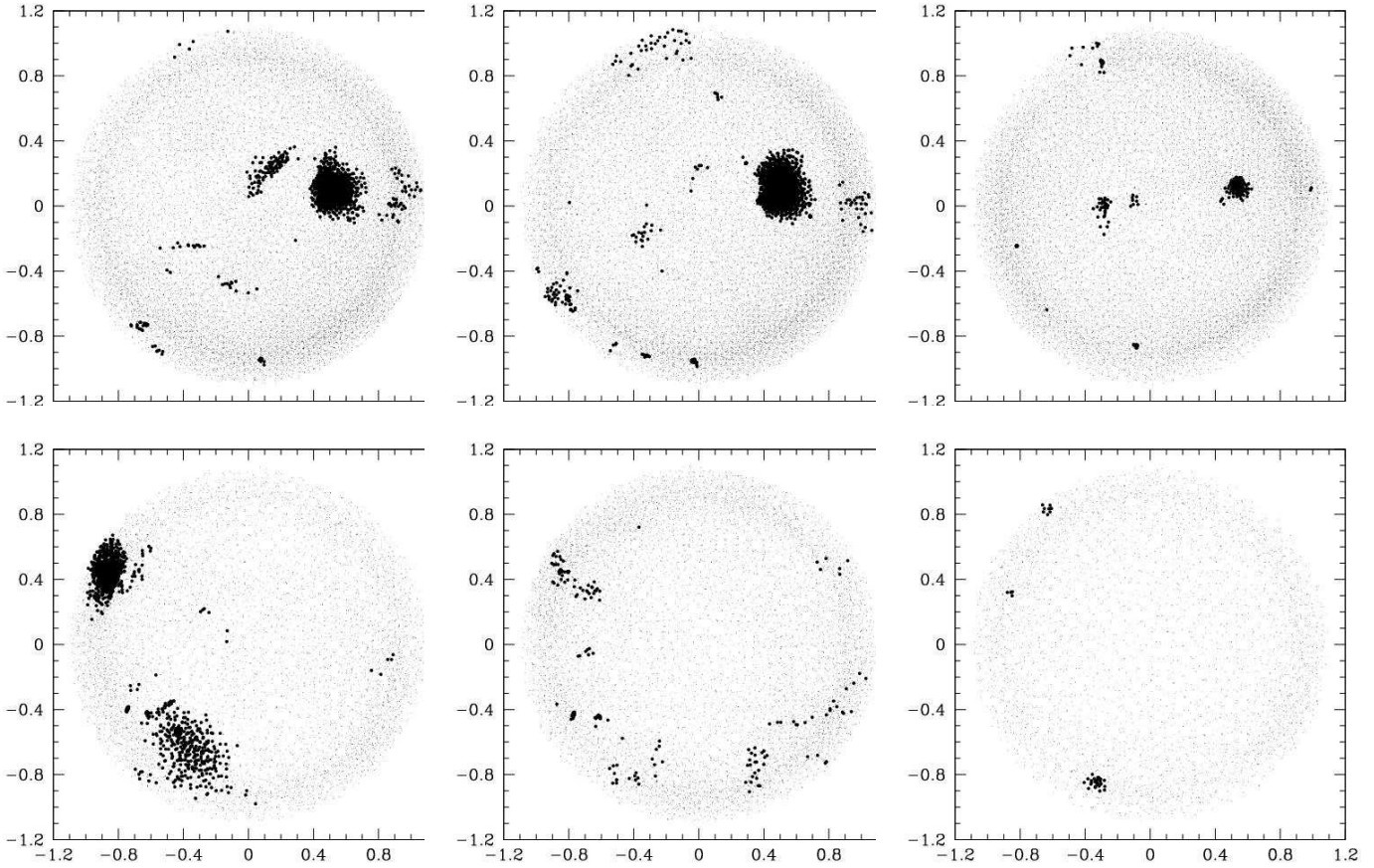


Figure 5. The distribution of gas particles in the outskirts ($0.9 < R/R_{\text{vir}} < 1.1$) of the Cluster (upper panel) and Group-3 (lower panels). Left, central and right panels are for the W1, W3 and W1+S100 models, respectively. Light and heavy points are for the gas particles whose entropy is above and below the value of 400 keV cm^2 for the Cluster and of 60 keV cm^2 for the Group-3. This plot demonstrates that such entropy values approximately mark the transition between clumpy and diffuse gas for the two simulated structures.

creasing the wind speed. Also, Fig. 5 shows that almost no signature of clumpy accretion is left in the ‘Group-3’ run. Comparing these results to those of the non-radiative runs shows that radiative cooling significantly reduces the entropy amplification. The main reason for this is that cooling increases gas density within accreting clumps and filaments, thus partially inhibiting the transition from clumpy to diffuse accretion. This effect can be appreciated by comparing the left panels of Fig. 4 with the left panels of Fig. 2. While the presence of cooling does not significantly change the entropy level of the accreting diffuse gas, it nevertheless allows residual low-entropy clumps in the outskirts to survive the pre-heating, thus lowering the overall amplitude of the entropy profiles.

An interesting characterisation of the effect of either increasing the wind speed or adding an entropy floor is obtained by comparing the star fraction with the corresponding specific extra energy involved by non-gravitational heating (see Table 2). Increasing the wind speed in the ‘Cluster’ runs has only a marginal effect on the entropy profiles, but it is quite effective in regulating cooling: the W3 model produces ~ 30 per cent fewer stars than the W1 model, bringing it into better agreement with observational data (e.g., Lin,

Mohr & Stanford 2003) which generally favour low stellar densities. Quite interestingly, strong winds are at least as efficient as the S100 model in preventing overcooling, while requiring a lower amount of extra energy per gas particle. This highlights the different ways in which winds and an entropy floor affect the thermodynamics of the diffuse baryons. The former acts locally to increase the cooling time of the gas surrounding the star forming regions but it is inefficient in smoothing out the gas content of merging sub-halos. The latter provides a diffuse impulsive heating and provides for a much more efficient transition from smooth to diffuse accretion.

A further question we investigated is whether the different feedback and pre-heating schemes are able to violate the self-similarity of the entropy profiles as strongly as it is observed. For this purpose, we plot in Figure 7 the profiles of reduced entropy, $S(r)/T_{\text{mw}}(r)$, for the four simulated structures in different radiative runs. Since in this analysis we do not aim for a detailed comparison with observations, we here prefer to normalise the entropy to the mass-weighted temperature, T_{mw} , instead of using the emission-weighted temperature. The latter has been shown to provide an inaccurate measure for the spectroscopic temperature of the ICM that

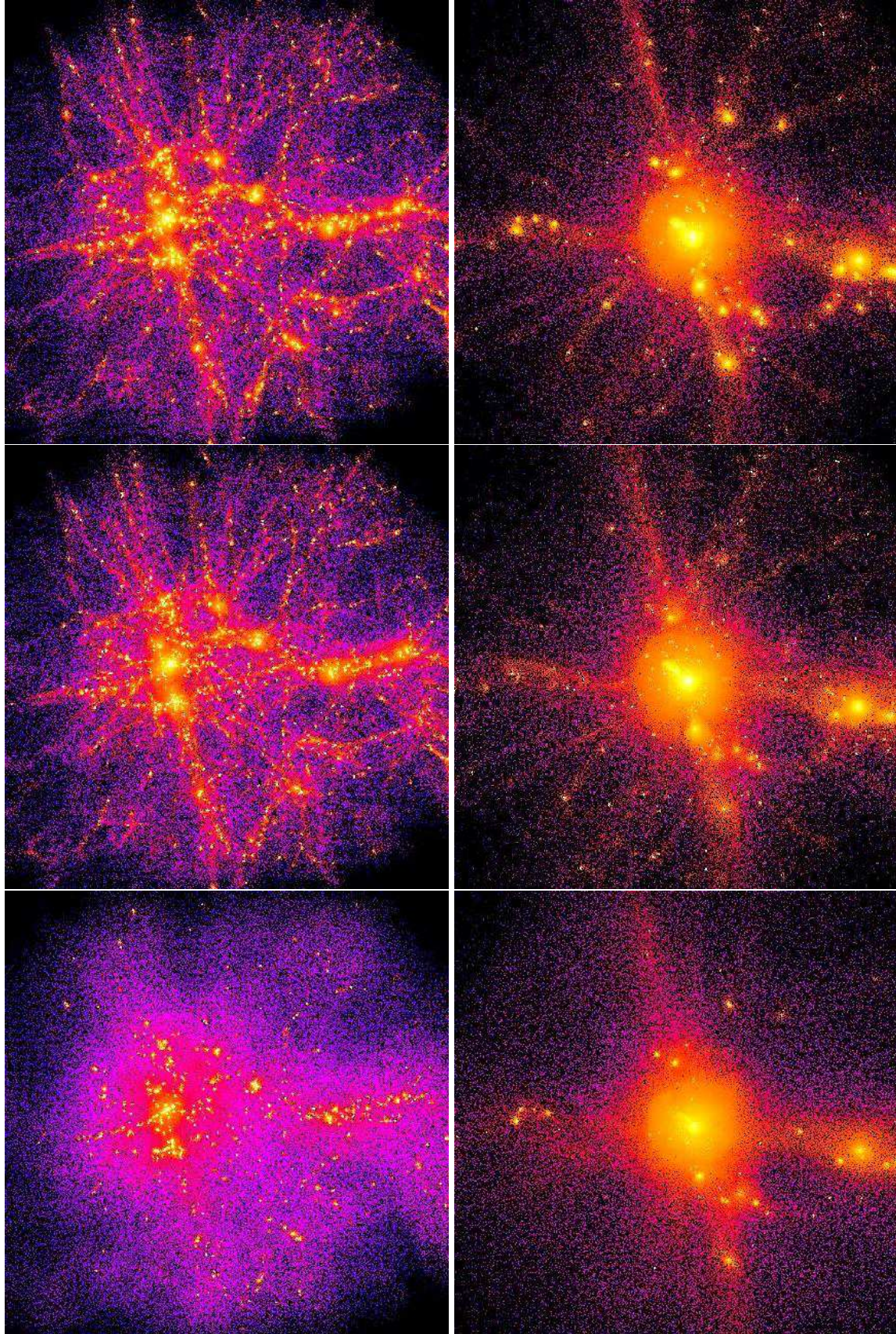


Figure 6. Maps of the gas density for the radiative runs of the Cluster. Upper, central and lower panels are for the W1, W3 and W1+S100 runs, respectively. Left and right panels are for the outputs at $z = 2$ and $z = 0$, respectively. At $z = 0$ the size of the box is $11.7 h^{-1} \text{Mpc}$, while at $z = 2$ it corresponds to $17.5 h^{-1} \text{Mpc}$ comoving. The small white knots mark the ‘‘galaxies’’, i.e. the places where high density gas is undergoing cooling and star formation.

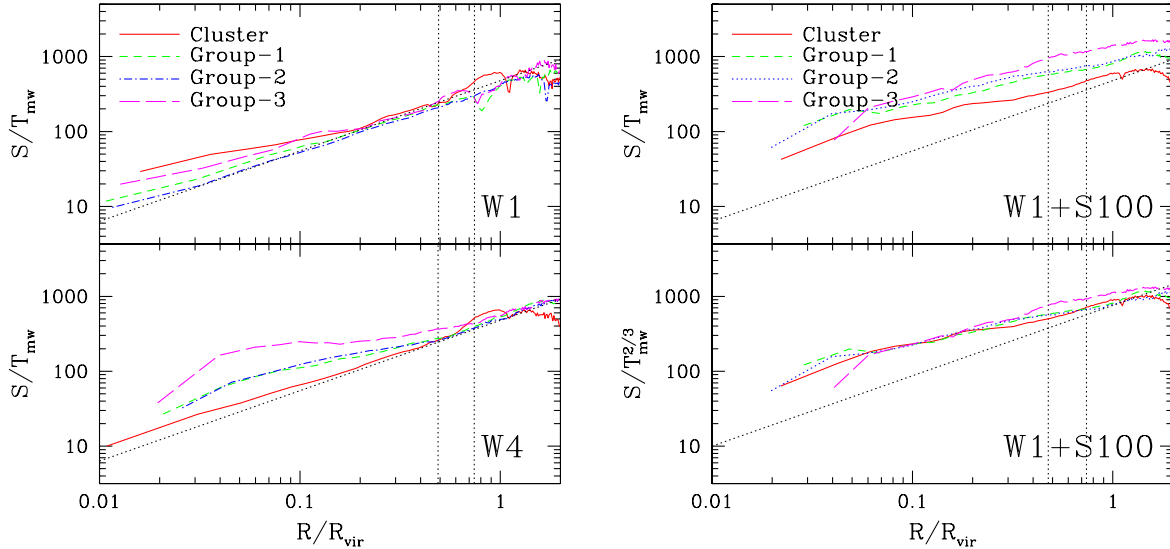


Figure 7. The profile of reduced entropy for the radiative runs. The left panels and the upper right panel show the results for the runs with wind velocity $v_W = 341 \text{ km s}^{-1}$ (W1 runs) and 837 km s^{-1} (W4 runs), and for the W1 runs that also include an entropy floor of 100 keV cm^2 (W1+S100), respectively. The profiles are scaled with the mass-weighted temperature, T_{mw} . The lower right panel shows the results of the W1+S100 runs, but with entropy profiles normalised according to the observed temperature scaling, $T_{\text{mw}}^{2/3}$. In all panels, the straight dotted line marks the slope $S \propto R^{0.95}$ which is the best-fit to the observed entropy profiles of Pratt & Arnaud (2004) and Piffaretti et al. (2005). The vertical dotted lines are for r_{200} and r_{500} of the Cluster.

is observationally inferred from X-ray spectra (e.g., Mathiesen & Evrard 2001; Mazzotta et al. 2004; Vikhlinin 2005). Although cooling, star formation and SN feedback are likely to introduce characteristic scales in the ICM thermodynamics, all the W1 runs have remarkably self-similar entropy profiles, over the whole range of resolved scales. However, for the W4 runs, the self-similarity is clearly broken in the central regions, while it is largely preserved at $R \gtrsim 0.5 R_{\text{vir}}$. Over the range of scales where self-similarity is preserved, the slope of the entropy profiles is always consistent with the $S \propto R^{0.94}$ behaviour found by Pratt & Arnaud (2004) and Piffaretti et al. (2005) from their analysis of groups and clusters observed with XMM-Newton.

As expected, only the S100 entropy floor generates an appreciable breaking of self-similarity in the outer regions of the simulated structures. In the lower right panel of Figure 7 we show the entropy profiles rescaled according to $T_{\text{mw}}^{2/3}$, which is consistent with the scaling suggested by observational data. Quite ironically, while this time we are able to reproduce the scaling with temperature of the normalisation of the profiles, we lose the agreement with the radial slope, which is significantly shallower than the observed one. We note here that an accurate derivation of the ICM entropy profiles from observations requires properly resolving both the gas density profiles and the temperature profiles. While different authors generally agree on the radial run of gas density, the temperature profiles are still a matter of vigorous debate. For instance, both ASCA (e.g., Markevitch et al. 1998; Finoguenov et al. 2001) and Beppo-SAX (e.g., De Grandi & Molendi 2002) consistently find decreasing profiles, at least for $R \gtrsim 0.2 R_{180}$ (cf. also White 2000). However, Pratt & Arnaud (2003, 2004) find profiles consistent with being isothermal, at least outside the cooling re-

gions. More recently, Piffaretti et al. (2005) and Vikhlinin et al. (2004) find decreasing outer profiles from XMM-Newton and Chandra data, respectively. While we do not intend to enter this debate here, we note that shallower entropy profiles should be obtained from data when the corresponding temperature profiles have a negative outer gradient.

4 DISCUSSION AND CONCLUSIONS

In this paper, we have analysed hydrodynamical simulations of the formation of one galaxy cluster and three galaxy groups, with the main aim of studying the ability of different models of non-gravitational heating to cause an amplification of entropy generation by accretion shocks as a consequence of a transition from clumpy to smooth accretion (e.g. Voit & Ponman 2003). For this purpose, we have carried out non-radiative simulations as well as simulations with cooling and star formation, and combined those with two different models for non-gravitational heating. The extra heating has been supplied in two different forms: (a) by imposing an entropy floor at $z_h = 3$; (b) by including the effect of galactic winds (Springel & Hernquist 2003a) of different strengths in the runs with star formation.

The main results of our analysis give answers to the three questions posed in the Introduction, and can be summarised as follows.

- Smoothing the accretion pattern by pre-heating in simulations with non-radiative physics does indeed amplify the entropy generation out to the radius where accretion shocks are taking place. As predicted by semi-analytic models (Voit et al. 2003), this amplification is more pronounced for lower-

mass systems, because they accrete from smaller sub-halos whose gas content is more easily smoothed by extra heating.

(b) Radiative cooling reduces this amplification effect by a significant amount. Cooling has the effect of increasing the clumpiness of the accretion pattern, and thus acts against the smoothing induced by extra heating. We find that only our pre-heating model with an entropy floor $S_{\text{fl}} = 100 \text{ keV cm}^2$ generates a sizable entropy amplification out to the external regions, $R \gtrsim 0.5 R_{\text{vir}}$, of group-sized halos.

(c) The heating from galactic winds is efficient in regulating star formation and in providing an increase of the ICM entropy in the central regions of groups. However, the winds have a negligible effect in smoothing the accretion pattern and thus do not trigger an appreciable entropy amplification effect. This result, which holds also for the strongest winds considered in our analysis, indicates that the role played by these winds tends to be fairly well localised around the star forming regions and therefore hardly affects the gas dynamics over the whole interior of dark matter halos.

Our results show that the temperature–entropy scaling provides powerful constraints on the physical nature of the energy feedback that affects the thermodynamic history of the diffuse baryons. Smoothing the gas accretion pattern within halos of forming galaxy clusters requires a rather non-local feedback, whose action should not only be that of preventing gas overcooling. The difficulties faced by our model for galactic winds suggest that we may miss a proper description of physics which is able to distribute the SN energy in the diffuse medium more efficiently (e.g. Kay et al. 2003, 2004, where cold galactic gas was impulsively heated to high temperature). Alternatively, this may be taken as an indication that other astrophysical sources of energy feedback are required. In this context, the most obvious candidate are probably AGN, whose effects should be taken into account self-consistently in future cosmological hydrodynamical simulations.

In this paper, we have not yet performed an in-depth comparison with observational data because we preferred to first provide a general interpretative framework for X-ray observations. However, a detailed comparison with observations in future work is very promising for extracting yet more information from the ICM thermodynamics. Particularly the increasing amount of high quality X-ray observations at the group scale (e.g. Finoguenov et al. 2004) together with the ever more sophisticated simulation models give a real hope that the intra-cluster baryons will remain an extremely useful tracer and will eventually allow us to understand the nature of feedback in groups and clusters.

ACKNOWLEDGEMENTS.

The simulations have been realized with CPU time allocated at the “Centro Interuniversitario del Nord-Est per il Calcolo Elettronico” (CINECA, Bologna), thanks to grants from INAF and from the University of Trieste. This work has been partially supported by the INFN Grant PD-51. We acknowledge useful discussions with Klaus Dolag, Giuseppe Murante and Luca Tornatore.

REFERENCES

Arnaud M., Evrard A.E., 1999, MNRAS, 305, 631
 Balogh M.L., Babul A., Patton D.R., 1999, MNRAS, 307, 463
 Bialek J.J., Evrard A.E., Mohr J.J., 2001, ApJ, 555, 597
 Borgani S., Governato F., Wadsley J., et al., 2001, ApJ, 559, L71
 Borgani S., Governato F., Wadsley J., et al., 2002, MNRAS, 336, 409
 Borgani S., Murante G., Springel V., et al., 2004, MNRAS, 348, 1078
 Bower R.G., 1997, MNRAS, 288, 355
 Bryan G.L., 2000, ApJ, 544, L1
 Cavalieri A., Menci N., Tozzi P., 1998, ApJ, 501, 493
 De Grandi S., Molendi S., 2002, ApJ, 567, 163
 Dos Santos S., Doré O., 2002, A&A, 383, 450
 Eke V.R., Navarro J., Frenk C.S., 1998, ApJ, 503, 569
 Evrard A.E., Henry J.P., 1991, ApJ, 383, 95
 Finoguenov A., Arnaud M., David L.P., 2001, ApJ, 555, 191
 Finoguenov A., Borgani S., Tornatore L., Böhringer H., 2003, A&A, 398, L35
 Finoguenov A., Davis D.S., Zimer M., Mulchaey J.S., 2004, ApJ, submitted
 Finoguenov A., Jones C., Böhringer H., Ponman T.J., 2002, ApJ, 578, 74
 Kaiser N., 1986, MNRAS, 222, 323
 Kaiser N., 1991, ApJ, 383, 104
 Kay S.T., Thomas P.A., Theuns T., 2003, MNRAS, 343, 608
 Kay S.T., Thomas P.A., Jenkins A., Pearce F.R., 2004, MNRAS, 355, 1091
 Lin Y.-T., Mohr, J.J., Stanford S.A., 2003, ApJ, 591, 749
 Mahdavi A., Finoguenov A., Böhringer H., Geller M.J., Henry J.P., 2005, ApJ, 622, 187
 Markevitch M., 1998, ApJ, 504, 27
 Markevitch M., Forman W. R., Sarazin C. L., Vikhlinin A., 1998, ApJ, 503, 77
 Mathiesen B.F., Evrard A.E., 2001, ApJ, 546, 100
 Mazzotta P., Rasia E., Moscardini L., Tormen G., 2004, MNRAS, 354, 10
 Muanwong O., Thomas P.A., Kay S.T., Pearce F.R., 2002, MNRAS, 336, 527
 Mushotzky R., Figueroa-Feliciano E., Loewenstein M., Snowden S.L., 2003 (preprint astro-ph/0302267)
 Navarro J.F., Frenk C.S., White S.D.M., 1995, MNRAS, 275, 720
 Navarro J.F., Frenk C.S., White S.D.M., 1997, ApJ, 490, 493
 Piffaretti R., Jetzer Ph., Kaastra J.S., Tamura T., 2005, A&A, 433, 101
 Ponman T.J., Cannon D.B., Navarro J.F., 1999, Nature, 397, 135
 Ponman T.J., Sanderson A.J.R., Finoguenov A., 2003, MNRAS, 343, 331
 Pratt G.W., Arnaud M., 2003, A&A, 408, 1
 Pratt G.W., Arnaud M., 2005, A&A, 429, 791
 Rosati P., Borgani S., Norman C., 2002, ARAA, 40, 539
 Sanderson A.J.R., Ponman T.J., Finoguenov A., Lloyd-Davies E.J., Markevitch M., 2003, MNRAS, 340, 989
 Salpeter E.E., 1955, ApJ, 121, 161
 Springel V., Hernquist L., 2002, MNRAS, 333, 649
 Springel V., Hernquist L., 2003a, MNRAS, 339, 289 (SH03)
 Springel V., Hernquist L., 2003b, MNRAS, 339, 312
 Springel V., Yoshida N., White S.D.M., 2001, NewA, 6, 79
 Tornatore L., Borgani S., Springel V., Matteucci F., Menci N., Murante G., 2003, MNRAS, 342, 1025
 Tozzi P., Norman C., 2001, 546, 63
 Vikhlinin A., 2005, ApJ, submitted (preprint astro-ph/0504098)
 Vikhlinin A., Markevitch M., Murray S.S., Jones C., Forman W., Van Speybroeck L., 2004, ApJ, submitted (preprint astro-ph/0412306)
 Voit, G.M. 2005, Rev. Mod. Phys., Jan. 2005 issue (preprint astro-ph/0410173)

Voit G.M., Balogh M.L., Bower R.G., Lacey C.G., Bryan G.L., 2003, *ApJ*, 593, 272

Voit G.M., Bryan G.L., 2001, *Nat*, 414, 425

Voit G.M., Bryan G.L., Balogh M.L., Bower R.G., 2002, *ApJ*, 576, 601

Voit G.M., Ponman T.J., 2003, *ApJ*, 594, L75

White D.A., 2000, *MNRAS*, 312, 663

Wu X.-P., Xue Y.-J., 2002, *ApJ*, 569, 112